J. Biochem. 125, 177-185 (1999)

Formation of the Myosin·ADP·Gallium Fluoride Complex and Its Solution Structure by Small-Angle Synchrotron X-Ray Scattering

Shinsaku Maruta,*,[1] Yasuo Uyehara,* Kazuaki Homma,* Yasunobu Sugimoto,† and Katsuzo Wakabayashi†

Department of Bioengineering, Faculty of Engineering, Soka University, Hachioji, Tokyo 192-8577; and †Department of Biophysical Engineering, Faculty of Engineering Science, Osaka University, Toyonaka, Osaka 560-8531

Received July 7, 1998; accepted October 8, 1998

In the presence of MgADP, a novel phosphate analogue of gallium fluoride (GaFn) forms a ternary complex with the myosin subfragment-1 (S-1), in the same way that has been previously reported with aluminum fluoride (AlF_4^-), beryllium fluoride (BeFn), scandium fluoride (ScFn), and vanadate (Vi), and this complex formation may mimic different states along the ATPase kinetic pathway. This novel complex has been characterized and compared with other complexes to ascertain whether it forms a transition-state analogue of myosin ATPase. The complex formed quickly, although several times slower than the BeFn complex. The half-life of the myosin·ADP·GaFn complex was about 50 h at 4°C. The formation of the myosin·ADP·GaFn complex was accompanied by an increase in tryptophane fluorescence, similar to that observed upon the addition of ATP, but slightly lower than that of the M·ADP·P_i complex. Upon addition of GaFn to acto-myosin·ADP, actomyosin did not dissociate, and the S-1·ADP·GaFn complex was scarcely decomposed by actin, like the AlF_4^- and ScFn complexes but unlike the BeFn and Vi complexes. The conformations at the localized region of SH1, SH2, and RLR, which are very accessible to the binding of ATP, were studied by fluorescent labeling and chemical modification, and the results suggested that these conformations are very similar to that of the M**·ADP·P_i state. Small-angle X-ray solution scattering showed that the radius of gyration value decreases by about 3 Å when S-1 forms an S-1·ADP·GaFn complex, suggesting that the shape of the complex becomes compact or rounded in shape, similar to that in the presence of ATP or complexes with other phosphate analogues, and thus mimics the myosin**·ADP·P_i state closely. The overall results may indicate that the complex mimics a somewhat different transient state from that of other complexes but has a similar global conformation along the ATPase kinetic pathway.**

Key words: energy transduction, myosin ATPase, phosphate analogue, transition state complex, X-ray scattering.

The energy for muscle contraction is derived from the hydrolysis of MgATP by myosin and the activation of this process by actin. Recent crystallographic studies of head skeletal muscle myosin (*1*) and the motor domain of *Dictyostelium* myosin (*2*) have shown the exact structure of the ATP- and actin-binding sites. A possible molecular model of cross-bridge cycling was proposed based upon the structure of S-1 determined by Rayment *et al.* (*3*). However, the mechanistic details at the molecular level, *i.e.*, how ATP chemical energy is converted to energy for the contractile machinery, remain unclear. Numerous biochemical and physical studies have indicated that the myosin head changes its global conformation and its localized flexible region during the series of steps constituting the ATPase cycle. The conformational changes at the localized regions are reflected by alterations in intrinsic tryptophane fluorescence (*4*), reactivity to chemical modification of several specific amino acid residues SH1, SH2 (*5-7*) and a reactive lysine residue (*8, 9*). Overall shape change of the myosin head during ATP hydrolysis was first shown by using small-angle X-ray scattering (*10*). During the contractile cycle, myosin forms a series of intermediates which may be directly related to such conformational changes of the myosin head. Studying the sequential conformational changes is very important in clarifying the mechanism of energy transduction. However, the intermediates have only a limited lifetime and it is difficult to isolate each ATPase reaction intermediate for biochemical and biophysical analysis. Therefore, stable analogues that

[1] To whom correspondence should be addressed. Fax: +81-426-91-9312, Phone: +81-426-91-9443, E-mail: shinsaku@t.soka.ac.jp

Abbreviation: ABDF, 4-fluoro-7-sulfamoylbenzofurazan; AlF_4^-, aluminum fluoride; BeFn, beryllium fluoride; DTT, dithiothreitol; GaFn, gallium fluoride; MIANS, 2-(4′-maleimidylanilino)naphthalene-6-sulfonic acid; PP_i, pyrophosphate; RLR, highly reactive lysine residue; S-1, myosin subfragment-1; S-1Dc, myosin head from *Dictyostelium discoideum* myosin II; ScFn, scandium fluoride; SDS-PAGE, sodium dodecyl sulfate polyacrylamide gel electrophoresis; TNBS, trinitrobenzene sulfonate; Vi, vanadate.

correspond to these species are useful in analyzing their structures.

Goodno (*11*) demonstrated that orthovanadate (Vi), a well known phosphate analogue, forms a stable ternary complex with myosin and ADP (myosin·ADP·Vi), and the complex may mimic the steady-state intermediate, M**·ADP·P_i, of the ATPase cycle. Recently it was shown that the phosphate analogues of fluorometals, aluminum fluoride (AlF_4^-), beryllium fluoride (BeFn), and scandium fluoride (ScFn), also form stable ternary complexes, *i.e.*, myosin·ADP·AlF_4^- (*12-14*), myosin·ADP·BeFn (*12-15*), and myosin·ADP·ScFn (*16*). The differences in the interaction with actin and the localized conformation of the complexes suggested that each complex may mimic distinct reaction intermediates of the myosin ATPase cycle (*13*). Moreover, recent crystallographic studies (*2, 17*) have revealed differences between the ternary complexes (AlF_4^-, BeFn, Vi) in the conformation of the COOH-terminal segment of the truncated myosin head from *Dictyostelium discoideum* myosin II (S-1Dc).

Nevertheless, discrepancies exist in the conformational data obtained from numerous biochemical and crystallographic studies. The most significant difference is that the crystal structure of the truncated S-1Dc·ADP·BeFn ternary complex is almost identical to that seen in the absence of nucleotide (*2*). In contrast, in solution, the skeletal muscle S-1·ADP·BeFn complex showed the formation of a complex similar to M**·ADP·P_i, reflected by tryptophane fluorescence enhancement, alteration of reactivities at the reactive amino acid residues (SH1, SH2, and RLR), and interaction with actin (*13-15, 18, 19*). It is difficult to compare directly the crystal structure with the biochemical data of skeletal muscle myosin. This may be either because the crystal structure was obtained using the truncated *Dictyostelium* myosin head or because chemically-modified skeletal muscle S-1 may not reflect a realistic conformation in solution, especially at the flexible loops of the actin binding site, the SH1-SH2 region, and the possible hinge region between the motor domain and the regulatory domain. A crystal structure directly comparable to the structure of skeletal S-1 in solution has not yet been elucidated.

In contrast, X-ray solution scattering measurement is a useful method to detect directly any large-scale changes in molecular structure in solution during functioning under physiological conditions. Wakabayashi *et al.* succeeded in observing the compact or rounded shape of S-1 in the presence of ATP and S1·ADP·P_i analogue (AlF_4^-, BeFn, and Vi) complexes, which differed from that of S-1 in the absence of nucleotide (*10, 20*).

Recently Park *et al.* (*21*) demonstrated that the new phosphate analogue, gallium fluoride (GaFn), also forms a stable ternary complex with myosin and ADP, and the conformation at the cleft containing SH1 (Cys707) and Trp510 of the complex was different from those of the other ternary complexes. In the present study, we have examined localized and global structures of the S-1·ADP·GaFn complex to see what the structure of the new complex is and whether it differs from the previously reported complexes. The effect of actin on the ternary complex was determined, and the conformations at the localized flexible regions (SH1, SH2, and RLR) of the S-1·ADP·GaFn complex were analyzed using chemical-modification fluorescence labeling. Small-angle synchrotron X-ray scattering was employed to study the global conformation of the new complex.

MATERIALS AND METHODS

Isolation of Skeletal Muscle Myosin Subfragment-1 (S-1)—Skeletal muscle myosin was prepared from chicken breast muscle according to the methods of Perry (*22*), and was digested by α-chymotrypsin to obtain subfragment-1, as reported by Weeds and Taylor (*23*).

Chemicals—ATP, ADP, dithiothreitol, Tris, NaF, $GaCl_3$, sodium orthovanadate, and ABDF were purchased from Wako Pure Chemicals. MIANS was purchased from Molecular Probes. [2,8-^{3}H]ATP (25 Ci/mmol) was purchased from Muromachi Chemicals.

ATPase Assay—Mg^{2+}-ATPase measurements were carried out in the presence of 2 mM ATP, 120 mM NaCl, 30 mM Tris-HCl, pH 7.5, 5 mM $MgCl_2$, and in the presence or absence of 0.1 mM $GaCl_3$, 50 mM NaF, and 1 mM ADP at 25°C. EDTA(K^+)-ATPase assay was performed in the presence of 2 mM ATP, 0.5 M KCl, 30 mM Tris-HCl, pH 7.5, and 5 mM EDTA. The reaction was stopped by addition of 10% trichloroacetic acid, and the released P_i was determined by the method of Youngburg and Youngburg (*24*).

Fluorescent Labeling of Reactive Cysteine Residues—Fluorescent labeling of SH1 (Cys707) with ABDF was performed according to Hiratsuka (*25*). The ratio of incorporated ABD group/S-1 was estimated from the absorption spectrum using an extinction coefficient of $6,000 \pm 500$ $M^{-1} \cdot cm^{-1}$ at 378 nm. SH2 (Cys697) was labeled with MIANS according to Hiratsuka (*26*). Prior to modification of SH2, SH1 was modified with the reversible blocking reagent 2,4-dinitro-1-fluorobenzene (*27*). The stoichiometry of the MIANS groups incorporated into S-1 was estimated from the difference in absorption spectra between S-1 labeled at Cys697 with MIANS and control S-1, using an extinction coefficient of 1.7×10^4 $M^{-1} \cdot cm^{-1}$ at 325 nm (*26*).

Fluorescence Measurements—These were performed using a spectrofluorometer (RF-5000, Shimadzu) at 20°C. S-1 labeled by MIANS was excited at 330 nm, and emission was monitored at 420 nm. S-1 labeled by ABDF was excited at 390 nm, and emission was monitored at 500 nm. To monitor the intrinsic tryptophane fluorescence of the myosin·ADP·GaFn complex at 335 nm, the complex was excited at 300 nm.

Trinitrophenylation of S-1·ADP·P_i Analogue Complexes—To measure the time course of trinitrophenylation of skeletal S-1 with ATP analogue, 12 μM S-1 was combined with trinitrobenzene-sulfonate (0.25 mM) at 25°C in 100 mM imidazole-HCl, pH 7.0, 0.5 M KCl, and 5 mM $MgCl_2$ (or 5 mM $CaCl_2$) in the presence of 2 mM ATP, 2 mM ADP, or 2 mM ADP, 0.1 mM $GaSO_4$, and 0.5 M NaF. The time course of trinitrophenylation was monitored at 345 nm using a spectrophotometer with a thermostated cell (Shimadzu UV 2200).

SDS-PAGE—Electrophoretic analysis was carried out on 7.5-20% polyacrylamide gradient gels. Peptide bands were visualized by staining with Coomassie Brilliant Blue. Molecular masses of the peptide bands were estimated by comparing their mobility with markers of known molecular weight.

X-Ray Solution Scattering—X-ray solution scattering

experiments were performed at 19°C with a small-angle diffractometer using synchrotron radiation at the Photon Factory (Tsukuba) by the method of Wakabayashi *et al.* (*10*). The scattering curves from S-1 samples were recorded with a one-dimensional position sensitive detector up to the scattering length $S = 0.02$ Å^{-1} [$S = 2 \sin \theta/\lambda$ where 2θ is the scattering angle and λ is the wavelength of X-rays (1.54 Å)] at a camera length of 2.33 m. The protein concentration used varied from 3 to 12 mg/ml. Each sample was centrifuged just before X-ray experiments to remove any aggregates. As control experiments, the S-1 samples without nucleotide and in the presence of MgATP were measured. The apparent radius of gyration (Rg) was calculated from the slope of the linear region in the Guinier plot [$\log[I(S)]$ *vs.* S2 (superscript)] of scattering intensity data. The true Rg value was obtained by extrapolating the apparent values to zero protein concentration.

RESULTS

Inhibition of ATPase Activity of S-1 by GaFn—The formation of the ternary complex of myosin·ADP·GaFn was monitored by measuring the inhibition of ATPase activity. As shown in Fig. 1, Mg-ATPase activity of the skeletal muscle myosin subfragment-1 (S-1) was strongly inhibited in the presence of both ADP and gallium fluoride (GaFn) in a time-dependent manner. Some inhibition was also observed in the absence of additional ADP due to the production of ADP by the hydrolysis of ATP during the S-1 ATPase reaction. Previously, we have shown that the Mg-ATPase activity of myosin is inhibited by aluminum fluoride (AlF_4^-) and beryllium fluoride (BeFn) in a similar time-dependent manner (*13*). AlF_4^- or BeFn is trapped in the active site due to the formation of the stable myosin·ADP·AlF_4^- or BeFn complex in which AlF_4^- or BeFn behaves as a phosphate analogue. Crystallographic studies of *Dictyostelium* S-1 have demonstrated directly that the phosphate analogues coordinate at the γ-phosphate binding site (*2*). The result shown in Fig. 1 suggests the formation of an analogous stable S-1·ADP·GaFn complex in which ADP is also trapped at the active site.

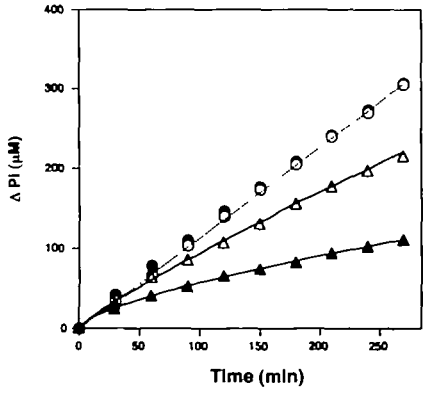

Fig. 1. **Inhibition of skeletal muscle myosin subfragment-1 (S-1) Mg^{2+}-ATPase activity by GaFn.** S-1 (2 μM) was preincubated for 5 min in 120 mM NaCl, 5 mM $MgCl_2$, 30 mM Tris-HCl, pH 7.5 (○), and 0.1 mM $GaCl_3$, 50 mM NaF, 1 mM ADP (▲), 0.1 mM $GaCl_3$, 50 mM NaF (△), or 1 mM ADP (●). The ATPase reaction was started by adding 2 mM ATP at 25°C.

The stable binding of ADP to S-1 in the presence of gallium fluoride was shown by gel filtration of the protein-nucleotide complex. S-1 was incubated with [^{3}H]ADP in the presence or absence of gallium fluoride and subjected to Sephadex G-50 gel filtration. As shown in Fig. 2, [^{3}H]ADP co-eluted with S-1 (first smaller peak) in the presence of gallium fluoride but not in its absence. These results suggested that the stable ternary complex of S-1·ADP·GaFn was formed. The amount of bound ADP was approximately 0.95 mol/mol site in the presence of GaFn from the quantitative analysis of protein and the count of [^{3}H]. The stability of the complex was examined by measuring the bound [^{3}H]ADP and recovery of ATPase activity after various times of dialysis (Fig. 3). The half-life of the S-1·ADP·GaFn complex was approximately 50 h, which is similar to that of AlF_4^-, as previously reported (*13, 14*). As a control, [^{3}H]ADP mixed with S-1 in the absence of GaFn was dialyzed out quickly within 1 h (data not shown). The ATPase activity was recovered accompanied by release of ADP. After dialysis for 170 h, almost complete recovery of ATPase and release of trapped ADP were observed.

Characterization of S-1·ADP·GaFn Complex—On addition of Mg-ATP, myosin quickly forms the M**·ADP·P_i intermediate, and this is characterized by an increase in the intrinsic tryptophane fluorescence intensity (*4*). We, therefore, examined whether myosin·ADP·GaFn forms the M**·ADP·P_i state by measuring the change in the intrinsic tryptophane fluorescence as a probe. As shown in Fig. 4, on addition of ATP, the tryptophane fluorescence intensity of S-1 quickly increased (approx. 16%) due to the formation of S-1**·ADP·P_i. After all the added ATP has been hydro-

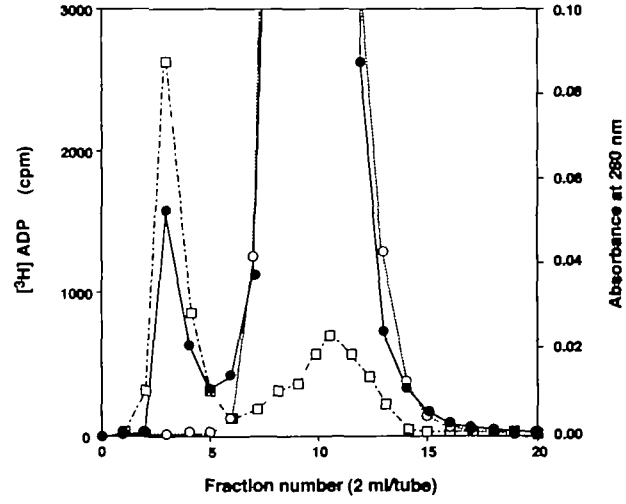

Fig. 2. **Separation of the S-1·ADP·GaFn ternary complex by Sephadex G-50 gel filtration.** S-1 (10 μM) in buffer containing 120 mM NaCl, 30 mM Tris-HCl, pH 7.5, and 2 mM $MgCl_2$ was preincubated for 1 h at 25°C with 100 μM [2,8-^{3}H]ATP (specific activity: 50,100 cpm/nmol). After ATP was completely hydrolyzed, 50 mM NaF and 0.1 mM $GaCl_3$ were added and the mixture was incubated for 2 h at 25°C. The mixture was applied to a 1.5×35 cm column of Sephadex G-50 equilibrated with 120 mM NaCl and 30 mM Tris-HCl pH 7.5. A 30 μl sample of each fraction was mixed with 5 ml of scintillation cocktail, and its radioactivity was measured in a Packard TRI-CARB 2700TR scintillation counter. ●: radioactivity in the presence of GaFn; ○: radioactivity in the absence of GaFn; □: absorbance at 280 nm.

lyzed, the fluorescence decreased due to the formation of S-1*·ADP. Subsequently, on addition of GaFn, fluorescence intensity increased slowly, accompanied by the formation of the S-1·ADP·GaFn complex. The maximum intensity was slightly lower and similar to the intensity of the S-1·ADP·BeFn complex, which differed from that of the S-1**·ADP·P_i by 20% (*13, 14*). These results suggest that the conformation of the S-1·ADP·GaFn complex is analogous to the ATPase reaction intermediate but not totally identical to S-1**·ADP·P_i.

Figure 5 shows the dissociation of acto-S-1 in the presence of ADP and various P_i analogues. Acto-S-1 dissociated immediately in the presence of ADP and BeFn. ADP and Vi also dissociate acto-S-1 about 10 times slower than in the presence of ADP and BeFn. In contrast, acto-S-1 did not dissociate at all in the presence of ADP and GaFn under these experimental conditions. This is consistent with the earlier findings that ADP and AlF_4^- did not dissociate at all for smooth muscle S-1 (*13*) and dissociated very slowly for skeletal muscle S-1 (*14*). We have shown previously that [^{14}C]ADP is not trapped into acto-S-1 in the presence of AlF_4^-. This result suggests that in the presence of actin, GaFn barely binds to the ATPase site of S-1, similar to AlF_4^-. It is likely that either actin or GaFn can bind to S-1·ADP, but not both. We examined the effect of actin on the S-1·ADP·GaFn complex. The time-dependent release of

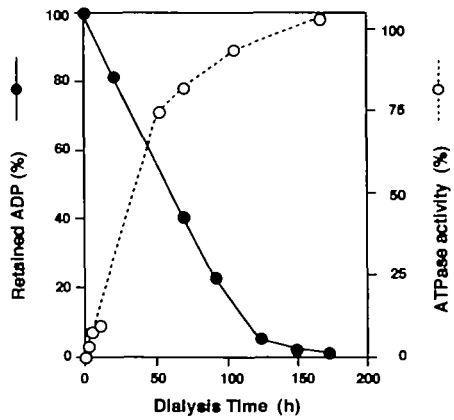

Fig. 3. **Time course of [^{3}H]ADP release from S-1·[^{3}H]ADP·GaFn and recovery of ATPase activity.** S-1 (10 μM) was preincubated with 0.1 mM [^{3}H]ATP at 25°C in the solution of 120 mM NaCl, 30 mM Tris-HCl, pH 7.5, and 2 mM $MgCl_2$. After ATP was completely hydrolyzed, 50 mM NaF and 0.1 mM $GaCl_3$ were added and the mixture was incubated for 180 min at 25°C. The complexes were purified by passage through a Sephadex G-50 column, then dialyzed against 300 ml of 120 mM NaCl and 30 mM Tris-HCl, pH 7.5, at 4°C. Aliquots were removed and immediately assayed for EDTA(+K)-ATPase activity and radioactivity.

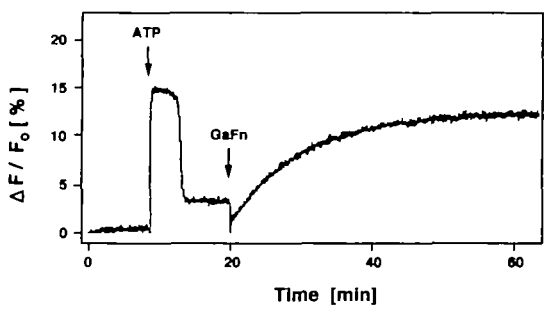

Fig. 4. **Incremental time course of intrinsic tryptophane fluorescence intensity of S-1 induced by ADP/GaFn.** To S-1 (1 μM) in 50 mM KCl, 30 mM Tris-HCl, pH 7.5, and 2 mM $MgCl_2$, 10 mM ATP was added at 25°C. After ATP was completely hydrolyzed, 0.1 mM gallium fluoride (GaFn) was added, and the change in the fluorescence intensity was monitored. The excitation and emission wavelengths were 300 and 335 nm, respectively.

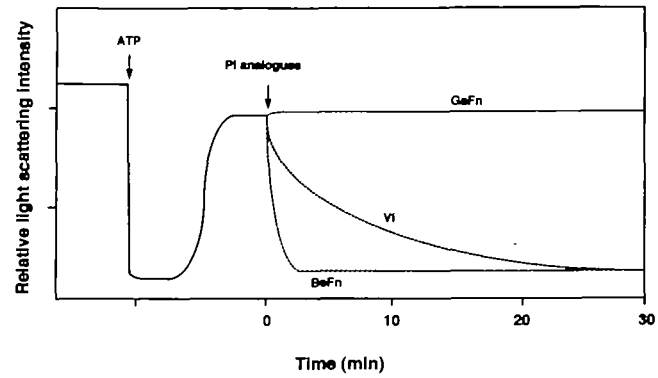

Fig. 5. **Dissociation of acto S-1 by ADP/GaFn.** Acto S-1 dissociation was monitored by the change in light scattering intensity at 500–550 nm in a solution of 1 μM S-1, 2 μM F-actin, 120 mM NaCl, 30 mM Tris-HCl, pH 7.5, and 5 mM $MgCl_2$ (or 5 mM $CaCl_2$) at 25°C.

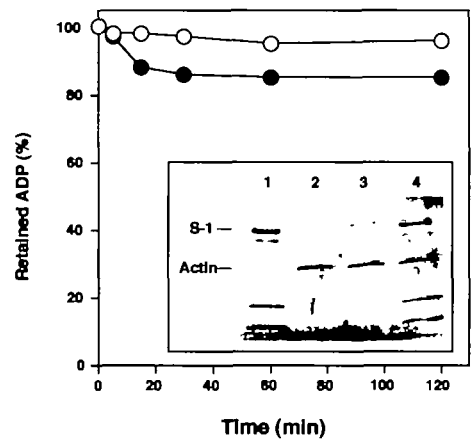

Fig. 6. **Time course of ADP release from skeletal muscle myosin S-1·ADP·GaFn complex.** The ternary complex was formed by incubation of 20 μM S-1 with 40 μM [^{3}H]ADP and 0.1 mM GaFn for 2 h at 25°C, then purified by passage through a Sephadex G-50 column. ADP retained in the ternary complex was determined by counting the [^{3}H]ADP remaining after removal of free [^{3}H]ADP released by actin. The reaction was started by adding ATP (○) or ATP and F-actin (●) to the solution containing the ternary complex. After 5, 15, 30, 60, and 120 min, Dowex 1×8 anion-exchange resin was added to the solution to remove ADP released from the ternary complex. The resin was quickly removed by centrifugation, and the [^{3}H]ADP retained in the S-1 in the solution was counted. Conditions: 8 μM S-1, 40 μM F-actin, 40 μM ATP, 0.12 M NaCl, and 30 mM Tris-HCl, pH 7.5, at 25°C. Inset: SDS-PAGE of the supernatant after ultracentrifugation of the S-1·ADP·GaFn complex in the presence of F-actin. The S-1·ADP·GaFn complex was prepared as described above. S-1 and the ternary complex were incubated with F-actin, then centrifuged for 1 h at 140,000×*g*. The supernatant was analyzed by SDS-PAGE using a 7.5–20% acrylamide gradient gel. Lane 1, S-1; lane 2, F-actin; lane 3, S-1 and F-actin; lane 4, S-1·ADP·GaFn complex and F-actin.

[^{3}H]ADP from the ternary complex on addition of actin was also examined. As shown in Fig. 6, ADP was not released significantly on addition of actin. The interaction of actin with the S-1·ADP·GaFn complex was also analyzed using an ultracentrifuge. The isolated S-1·ADP·GaFn from the addition of excess ADP and GaFn was incubated with actin and subsequently ultracentrifuged. The S-1 remaining in the supernatant was analyzed by SDS-PAGE and the results are shown in the inset of Fig. 6. From the densitometric analysis of the gel, more than 90% of S-1 was still in the supernatant (Fig. 6 inset: lane 4), suggesting that actin does not bind to the S-1·ADP·GaFn complex. This is consistent with the results produced by the first method and suggests that actin does not significantly decompose the ternary complex. These results suggest that the S-1·ADP·GaFn complex is a weak binding state and its interaction with actin resembles that of the S-1·ADP·AlF_4^- complex.

Conformation of the S-1·ADP·GaFn Complex at the Localized Flexible Regions—The region of reactive cysteine residues, SH1 (Cys707) and SH2 (Cys697), is highly flexible and changes its conformation upon the binding of ATP and actin (*28–30*). The reactivity of the residues varies with the hydrolysis of ATP (*5–7*). Reisler *et al.* (*6*) demonstrated that the reactivity of Cys707 to thiol reagents is low in the S-1**·ADP·P_i complex and high in the S-1·ADP complex. The sequence of transient intermediates along the ATPase kinetic pathway may be reflected in the changing the conformation of this region. Hiratsuka (*25, 26*) showed that the conformational changes at the reactive thiols associated with ATP hydrolysis can be monitored by labeling SH1 and SH2 with a fluorescent probe, ABDF and MIANS, respectively. We labeled the reactive thiols of S-1 with a fluorescent probe according to Hiratsuka (*25, 26*) and monitored the change of the fluorescence intensity of the probe bound to the residue that accompanied the formation of the S-1·ADP·GaFn ternary complex.

Figure 7 shows the time course of fluorescence changes of S-1 labeled with ABDF at SH1 (ABD-S-1) on addition of ligands. On addition of ATP, the fluorescence intensity of ABD-S-1 increased by 110% due to the formation of a steady state. After all the added ATP has been hydrolyzed, the fluorescence decreased to the level seen in the presence of ADP. In the presence of ADP and GaFn, the fluorescence intensity increased, showing the formation of a ternary complex, and the maximum intensity attained to the level seen in the presence of ATP. These results suggest that, in the presence of ATP, the SH1 of the S-1·ADP·GaFn complex moves to the more hydrophobic protein interior as well as during the steady-state ATP hydrolysis.

Conformational change at the SH2 by the formation of the S-1·ADP·GaFn complex was also monitored by the fluorescence of MIANS-S-1. As shown in Fig. 8, when ATP

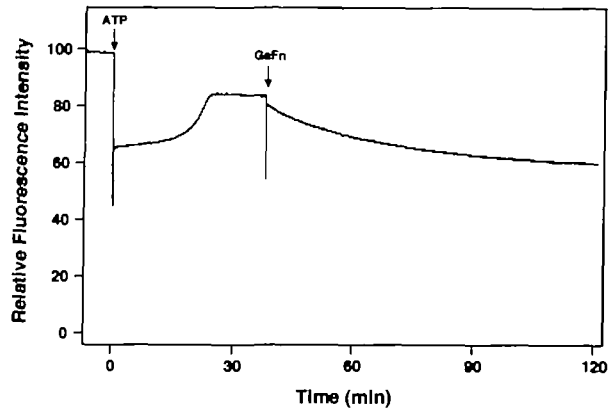

Fig. 8. **Time course of decrement of MIANS-S-1 fluorescence intensity induced by formation of the S-1·ADP·GaFn complex.** First, 1 mM ADP was added to a solution of 30 mM Tris-HCl, pH 7.5, 120 mM NaCl, 1 μM MIANS-S1, and 2 mM $MgCl_2$. Then 0.1 mM GaFn was added to the mixture. Excitation wavelength was 330 nm and emission was monitored at 420 nm.

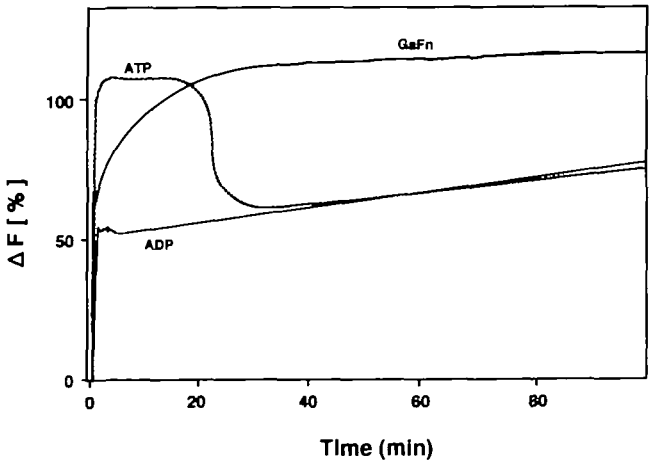

Fig. 7. **Time course of fluorescence change of ABD-S-1 on addition of ADP/GaFn.** The change in fluorescence intensity of ABD-S1 (1 μM) on addition of nucleotides or ADP/GaFn was monitored in a solution of 120 mM NaCl, 30 mM Tris-HCl, pH 7.5, and 2 mM $MgCl_2$ at 25°C. The excitation and emission wavelengths were 390 and 500 nm, respectively.

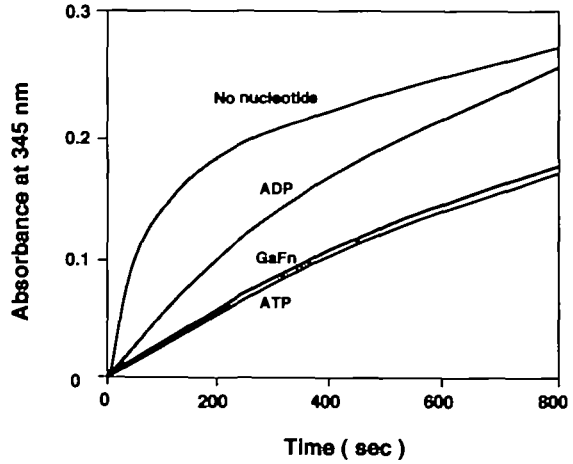

Fig. 9. **Time course of trinitrophenylation of the skeletal S-1·ADP·GaFn complex.** S-1 (12 μM) was treated with trinitrobenzenesulfonate (0.25 mM) at 25°C in 100 mM imidazole-HCl pH 7.0, 0.5 M KCl, 5 mM $MgCl_2$ in the presence of 2 mM ATP, 2 mM ADP, and 0.1 mM GaFn.

was added to MIANS-S-1, the fluorescence intensity decreased by 32% due to the formation of a steady state, consistent with the results reported by Hiratsuka (*26*). After all the added ATP had been hydrolyzed to ADP, the fluorescence intensity increased to the level seen in the presence of ADP. On addition of GaFn, the fluorescence intensity decreased to the same level as that seen in the presence of ATP due to the formation of the S-1·ADP·GaFn ternary complex. These results suggest that the formation of the S-1·ADP·GaFn complex causes a movement of SH2 towards the protein surface, similar to that seen in the presence of ATP.

The myosin head also contains one highly reactive lysine residue (RLR; Lys83), which is rapidly and stoichiometrically modified by TNBS (*31*). The trinitrophenylation of RLR markedly changes the enzymatic properties of myosin. In the presence of PP_i and nucleotide, the reactivity of the RLR is reduced (*8, 9, 32, 33*). The previous results suggest that the RLR region changes its conformation during ATP hydrolysis. We have examined the reactivity of RLR in the S-1·ADP·GaFn complex and compared it with that seen in the presence of ADP and ATP. As shown in Fig. 9, the rate of trinitrophenylation in the presence of ADP is reduced to approximately half of that in the absence of nucleotide, as previously reported. On addition of ATP, the trinitrophenylation is completely inhibited. Similarly, in the presence of ADP and GaFn, the trinitrophenylation of RLR is also completely abolished. It is suggested that the conformation at the RLR of the S-1·ADP·GaFn complex resembles that of the steady-state ATP hydrolysis. These results suggest that the conformations of the localized regions at SH1, SH2, and RLR on the S-1·ADP·GaFn complex are similar to those of the M**·ADP·P_i state.

Small Angle X-Ray Solution Scattering of the S-1·ADP·GaFn Complex—To study the global conformation of the S-1·ADP·GaFn complex, we utilized a small-angle synchrotron X-ray scattering technique using synchrotron radiation as an intense X-ray source. By measuring the radius of gyration (Rg) from the X-ray scattering curve, Wakabayashi *et al.* (*10*) clearly showed that the myosin head (S-1) assumes a more compact or rounded form in the presence of ATP, and that a similar compaction of the molecule occurs when ADP and Vi bind. The structures of the ternary complexes of S-1·ADP·AlF_4^- and S-1·ADP·BeFn have also been investigated by X-ray scattering. These complexes also have a more compact shape, comparable to that of S-1 in the MgATP solution (*20*). Such a change in shape is thought to be caused by a hinge-like bending motion between the catalytic and regulatory domains. The inspection of X-ray scattering data has revealed that the change in shape of S-1 that occurs in the presence of ATP is due to the formation of M**·ADP·P_i.

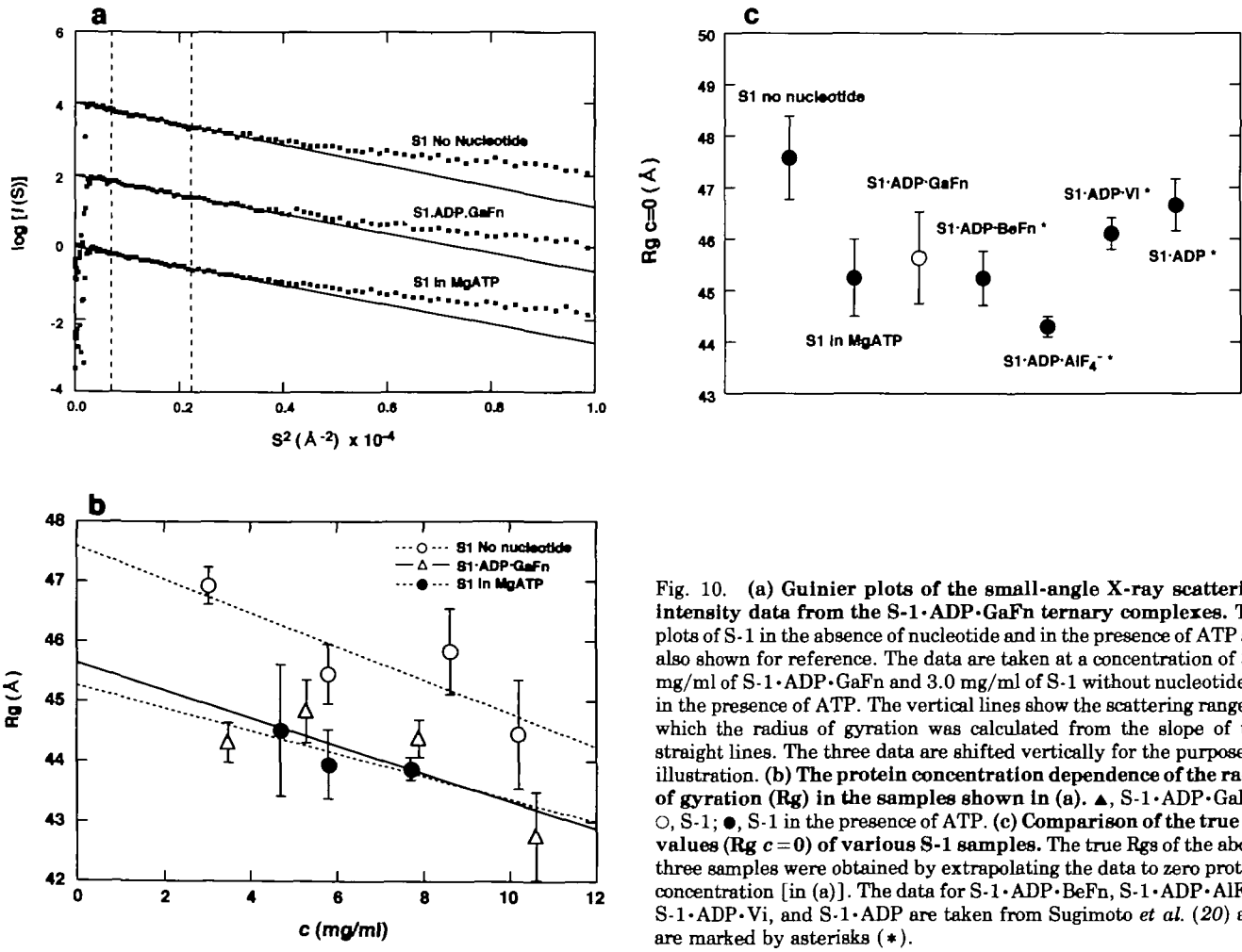

Fig. 10. **(a) Guinier plots of the small-angle X-ray scattering intensity data from the S-1·ADP·GaFn ternary complexes.** The plots of S-1 in the absence of nucleotide and in the presence of ATP are also shown for reference. The data are taken at a concentration of 3.5 mg/ml of S-1·ADP·GaFn and 3.0 mg/ml of S-1 without nucleotide or in the presence of ATP. The vertical lines show the scattering range in which the radius of gyration was calculated from the slope of the straight lines. The three data are shifted vertically for the purpose of illustration. **(b) The protein concentration dependence of the radii of gyration (Rg) in the samples shown in (a).** ▲, S-1·ADP·GaFn; ○, S-1; ●, S-1 in the presence of ATP. **(c) Comparison of the true Rg values (Rg $c=0$) of various S-1 samples.** The true Rgs of the above three samples were obtained by extrapolating the data to zero protein concentration [in (a)]. The data for S-1·ADP·BeFn, S-1·ADP·AlF_4^-, S-1·ADP·Vi, and S-1·ADP are taken from Sugimoto *et al.* (*20*) and are marked by asterisks (*).

We have also analyzed the solution structure of the S-1·ADP·GaFn complex by small-angle X-ray scattering and compared it with those of M**·ADP·P_i and other complexes. Figure 10a shows Guinier plots of the scattering data from this complex with those of S-1 in the absence of nucleotide and presence of ATP. They produced straight lines in the range of $S2 \leq 0.22 \times 10^{-4}$ Å^{-2}, showing no aggregates of the molecules in solution. The radius of gyration (Rg) was calculated from the slope of the straight lines in the Guinier plots in the range of $0.078 \times 10^{-4} \leq S2 \leq 0.223 \times 10^{-4}$ Å^{-2} and was plotted against the protein concentration c (Fig. 10b). As shown in Fig. 10b, when extrapolated to $c=0$ the true Rg value of the S-1·ADP·GaFn was about 45.5 Å, which is clearly less than that in the absence of nucleotide (48 Å) and comparable to that in the presence of MgATP (45 Å). When compared with the true Rg values of various complexes in Fig. 10c, the value of S-1·ADP·GaFn is much smaller than that of S-1·ADP (47 Å) but similar to those of S-1·ADP·BeFn and S-1·ADP·Vi (44.5–46 Å), and slightly larger than that of M**·ADP·P_i (a predominant intermediate state during ATP hydrolysis). Thus, the data clearly demonstrate that the S-1·ADP·GaFn complex has a compact or rounded shape similar to M**·ADP·P_i and other complexes with ADP·P_i analogues.

DISCUSSION

In the presence of Mg-ADP, the novel phosphate analogue GaFn forms a ternary complex of myosin·ADP·GaFn similar to the other fluorometals AlF_4^-, BeFn (*13–15*), and ScFn (*16*). We have previously demonstrated that these ternary complexes may mimic different steps along the ATPase kinetic pathway which accompanies the contractile cycle (*13, 19, 34*). It is useful to compare the GaFn complex with other well-studied complexes in order to identify the sequence of the ternary complexes through the ATPase cycle. It is clearly shown that ADP and GaFn are trapped stoichiometrically into the ATPase site of myosin as shown in Figs. 1 and 2. Park *et al.* quantitatively analysed Ga trapped into S-1 using inductive coupled plasma mass spectrometry and also showed direct evidence for the formation of the ternary complex (*35*). The inhibition of Mg-ATPase due to the formation of the ternary complex is slower than that of the BeFn complex, as previously reported (*14, 15*). The rate constant (k_{obs}) for the progressive inhibition of MgATPase activity of S-1, estimated from the semilogarithmic plot of the residual ATPase activity *versus* time, was 1.8×10^{-5} s^{-1}, corresponding to an apparent second-order rate constant (k_{app}) of 0.18 M^{-1}·s^{-1}. The latter second-order rate constant is several times lower than that observed with BeFn (*15*) but still about three times higher than that of ScFn (*16*). The stability of the S-1·ADP·GaFn complex at 4°C was followed by the release of trapped [^{3}H]ADP by dialysis of the complex. As shown in Fig. 3, the half-life of the complex was about 50 h, which is similar to half-life of AlF_4^- complex and several times shorter than that of BeFn complex (*14*). For the BeFn (*15*) and ScFn (*16*) complexes, the time dependence of the release was biphasic, first a fast release and second a slow release, suggesting the possibility that the ternary complex may be in equilibrium between two distinct conformations. A similar biphasic release was also observed for the GaFn complex, although the release was faster than that of the other complexes (Fig. 3).

The enhancement of tryptophane fluorescence associated with the formation of the GaFn complex showed a level of enhancement over that of the unliganded S-1 of ~12%. This is somewhat lower than that observed for the M**·ADP·P_i complex (~16%). We have previously demonstrated that the BeFn complex also showed a similar enhancement of tryptophane fluorescence (*13*). ^{19}F-NMR experiments clearly indicated that BeFn in the ternary complex has at least four species due to the different number of fluorines coordinating to beryllium (*36*). It is assumed that these species mimic different states of intermediates in ATPase cycle. Therefore, the lower enhancement of tryptophane fluorescence with the BeFn complex may depend on the mixture of the complexes, mimicking different states in the ATPase cycle. Although the existence of such species is not clear for the GaFn complex, the characteristic property of the tryptophane fluorescence enhancement is more similar to that of the BeFn complex than to those of the AlF_4^-, Vi, and ScFn complexes. The ternary complexes of the myosin·ADP·fluorometals previously studied are classified into two, one class for BeFn and the other for AlF_4^- and ScFn. For the former class, excess fluorometals dissociate from the acto-myosin·ADP complex very quickly. Alternatively, actin releases bound nucleotide and fluorometals in a comparable way to a normal product release process. Interestingly, the BeFn ternary complex showed a slightly lower tryptophane enhancement than that of M**·ADP·P_i in the presence of ATP. For a latter class of AlF_4^- and ScFn, it has been demonstrated that ADP/ScFn and ADP/AlF_4^- dissociate the acto-S1 much more slowly than ADP/BeFn does and alternatively show resistance to decomposition by actin. The tryptophane fluorescence enhancement by the BeFn ternary complex was almost the same or slightly higher than that of the M**·ADP·P_i complex. The difference in characteristic properties between the two classes of ternary complexes may be due to the existence of the different species mentioned earlier, or the difference in the geometry of the metallo-coordination. The coordinating ligand of BeFn has a tetrahedral geometry, but AlF_4^- and ScFn have an octahedral geometry.

Interestingly, vanadate, which is a well-known phosphate analogue with a bipyramidal geometry, showed properties intermediate between these two classes of complexes.

Although, GaFn has a tetrahedral geometry and its ternary complex showed a slightly lower tryptophane fluorescent enhancement, similar to BeFn, its interaction with actin was similar to that of AlF_4^-. As shown in Fig. 5, acto-myosin did not dissociate in the presence of ADP and GaFn, suggesting that GaFn cannot bind to the ATPase site of an acto-myosin·ADP complex. The S-1·ADP·GaFn ternary complex was not significantly decomposed by actin (Fig. 6 inset). Moreover, the ultracentrifuge analysis of the S-1·ADP·GaFn complex in the presence of actin also demonstrated that the complex did not coprecipitate with actin. These results strongly suggest that the S-1·ADP·GaFn complex mimics a weakly-bound state similar to the other ternary complexes but is not totally identical to the other complexes of AlF_4^-, BeFn, ScFn, and Vi in localized conformation. The conformation at the actin-binding site of GaFn complex may be somewhat different from that of M**·ADP·P_i.

Numerous biochemical and biophysical studies have suggested that the myosin head changes its localized conformations at the SH1-SH2 and RLR regions in a different way, leading to a global shape change during ATP hydrolysis. The region of the flexible SH1-SH2 residues is thought to act as an energy transduction loop through which intersite communication between the ATP- and actin-binding sites is transmitted. As shown in Figs. 7 and 8, the fluorescence of both probes at SH1 and SH2 of the S-1·ADP·GaFn complex showed intensity identical to that in the presence of ATP. We have previously shown that labeling by ABDF or MIANS did not affect the formation of ternary complexes of labeled S-1·ADP·AlF_4^- or ScFn (*37*). Moreover, the fluorescence intensity of the MIANS- or ABD-S-1·ADP·GaFn ternary complex was clearly different from that in the presence of only ADP. This indicates that ABD-S-1 and MIANS-S-1 form ternary complexes with ADP and GaFn. It is suggested that the conformation in the SH1-SH2 region of the complex is similar to the M**·ADP·P_i state rather than the M·ATP state. As shown in Fig. 9, in the presence of ADP and GaFn, the reactivity of RLR is reduced to a level identical to that in the presence of ATP, indicating that the conformation at the RLR region of the S-1·ADP·GaFn complex resembles that of the M**·ADP·P_i state. The results mentioned so far suggest that the localized conformations at Cys707 (SH1), Cys697 (SH2), and Lys83 (RLR) moeties of the S-1·ADP·GaFn complex are similar to those of the M**·ADP·P_i complex.

Recent X-ray solution scattering (*10*) and electron microscopic studies (*38-40*) have demonstrated that the myosin head changes its global conformation during ATP hydrolysis. The analysis of X-ray scattering data indicates that a conformational change of the myosin head in the presence of ATP is caused by a hinge-like bending motion between the catalytic and regulatory domains (*20*). The change in shape may be associated with the formation of the M**·ADP·P_i state. Although it is unknown whether the global change is directly related to the generation of the contractile force, as implied by the swinging neck-lever arm model (*41*), the change in shape may be related to localized conformational changes reflecting the energy transduction on the myosin head. The structures of S-1·ADP·AlF_4^-, S-1·ADP·BeFn and S-1·ADP·Vi, which are thought to be analogues of S-1·ADP·P_i, have also been analyzed by X-ray solution scattering (*20*). The results indicated that these ternary complexes have a compact or rounded shape, strongly suggesting that the ternary complexes mimic an intermediate state at or near M**·ADP·P_i in the ATPase cycle. In addition to these analogues, we have examined the structures of S-1·ADP·GaFn complex by X-ray scattering. As shown in Fig. 10, b and c, the radius of gyration value (Rg) of S-1·ADP·GaFn complex was almost identical to those of the other complexes. These results indicated that the global structure of the S-1·ADP·GaFn closely resembles that of S-1**·ADP·P_i. The Rg value of S-1·ADP·GaFn was clearly less than in the presence of ADP as well as in the absence of nucleotide, but any differences from those of S-1·ADP·BeFn and S-1·ADP·Vi are not conclusive because of the large standard deviation in the present X-ray work . The slight differences in Rg values among the ternary complexes listed in Fig. 10c may suggest that these complexes mimic different sequential intermediate states along the ATPase kinetic pathway. Alternatively, differences in a localized conformation in different ternary complexes may not be directly related to a global conformational change. These possibilities will be confirmed by more precise biochemical and physical techniques including X-ray scattering.

REFERENCES

1. Rayment, I., Rypniewski, W.R., Schmidt-Base, K., Smith, R., Tomchick, D.R., Benning, M.M., Winkelmann, D.A., Weenberg, G., and Holden, H.M. (1993) Three-dimensional structure of myosin subfragment-1: a molecular motor. *Science* **261**, 50-57
2. Fisher, A.J., Smith, C.A., Thoden, J.B., Smith, R., Sutoh, K., Holden, H.M., and Rayment, I. (1995) X-ray structures of the myosin motor domain of *Dictyostelium discoideum* complexed with MgADP·BeFx and MgADP·AlF_4^-. *Biochemistry* **34**, 8960-8972
3. Rayment, I., Holden, H.M., Whittaker, M., Yohn, C.B., Lorenz, M., Holmes, K.C., and Milligan, R.A. (1993) Structure of the actin-myosin complex and its implications for muscle contraction. *Science* **261**, 58-65
4. Werber, M.M., Szent-Gyorgyi, A.G., and Fasman, G.D. (1972) Fluorescence studies on heavy meromyosin-substrate interaction. *Biochemistry* **11**, 2872-2883
5. Harrington, W.F., Reisler, E., and Burke, M. (1975) An activation mechanism for ATP cleavage in muscle. *J. Supramol. Struct.* **3**, 112-124
6. Reisler, E., Burke, M., and Harrington, W.F. (1977) Reactivity of essential thiols of myosin. Chemical probes of the activated state. *Biochemistry* **16**, 5187-5191
7. Doung, A. and Reisler, E. (1989) Nucleotide-induced states of myosin subfragment 1 cross-linked to actin. *Biochemistry* **28**, 3502-3509
8. Mornet, D., Pantel, P., Bertrand, R., Audemard, E., and Kassab, R. (1980) Localization of the reactive trinitrophenylated lysyl residue of myosin ATPase site in the NH_2-terminal (27 k domain) of S1 heavy chain. *FEBS Lett.* **117**, 183-188
9. Komatsu, H., Emoto, Y., and Tawada, K. (1993) Half-stoichiometric trinitrophenylation of myosin subfragment 1 in the presence of pyrophosphate or adenosine diphosphate. *J. Biol. Chem.* **268**, 7799-7808
10. Wakabayashi, K., Tokunaga, M., Kohno, I., Sugimoto, Y., Hamanaka, T., Takezawa, Y., Wakabayashi, T., and Amemiya, Y. (1992) Small-angle synchrotron x-ray scattering reveals distinct shape changes of the myosin head during hydrolysis of ATP. *Science* **258**, 443-447
11. Goodno, C.C. (1979) Inhibition of myosin ATPase by vanadate ion. *Proc. Natl. Acad. Sci. USA* **76**, 2620-2624
12. Maruta, S., Henry, G.D., Sykes, B.D., and Ikebe, M. (1991) Formation of the stable smooth muscle myosin-ADP-AlF_3 complex and its analysis using ^{19}F-NMR. *Biophys. J.* **59**, 436a
13. Maruta, S., Henry, G.D., Sykes, B.D., and Ikebe, M. (1993) Formation of the stable myosin-ADP-aluminum fluoride and myosin-ADP-beryllium fluoride complexes and their analysis using ^{19}F NMR. *J. Biol. Chem.* **268**, 7093-7100
14. Werber, M.M., Peyser, Y.M., and Muhlrad, A. (1992) Characterization of stable beryllium fluoride, aluminum fluoride, and vanadate containing myosin subfragment 1-nucleotide complexes. *Biochemistry* **31**, 7190-7197
15. Phan, B. and Reisler, E. (1992) Inhibition of myosin ATPase by beryllium fluoride. *Biochemistry* **31**, 4787-4793
16. Gopal, D. and Burke, M. (1995) Formation of stable inhibitory complexes of myosin subfragment 1 using fluoroscandium anions. *J. Biol. Chem.* **270**, 19282-19286
17. Smith, C.A. and Rayment, I. (1996) X-ray structure of the magnesium(II)·ADP·vanadate complex of the *Dictyostelium discoideum* myosin motor domain to 1.9 Å resolution. *Biochemistry* **35**, 5404-5417
18. Phan, B., Faller, L.D., and Reisler, E. (1993) Kinetic and equilibrium analysis of the interactions of actomyosin subfrag-

ment-1·ADP with beryllium fluoride. *Biochemistry* **32**, 7712-7719
19. Maruta, S., Kambara, T., Sugimoto, Y., Takezawa, Y., Ikebe, M., and Wakabayashi, K. (1995) Chemical modification and small-angle x-ray scattering of myosin-ADP-fluorometal complexes. *Biophys. J.* **68**, 160a
20. Sugimoto, Y., Tokunaga, M., Takezawa, Y., Ikebe, M., and Wakabayashi, K. (1995) Conformational changes of the myosin heads during hydrolysis of ATP as analyzed by x-ray solution scattering. *Biophys. J.* **68**, 29s-34s
21. Park, S., Ajtai, K., and Burghardt, T.P. (1997) Mechanism for coupling free energy in ATPase to the myosin active site. *Biochemistry* **36**, 3368-3372
22. Perry, S.V. (1952) Myosin adenosin triphosphatase. *Methods Enzymol.* **2**, 582-588
23. Weeds, A.G. and Taylor, R.S. (1975) Separation of subfragment-1 isoenzymes from rabbit skeletal muscle myosin. *Nature* **257**, 54-56
24. Youngburg, G.E. and Youngburg, M.V. (1930) Phosphorus metabolism: I. A system of blood phosphorus analysis. *J. Lab. Clin. Med.* **16**, 158-166
25. Hiratsuka, T. (1993) Behavior of Cys707 (SH1) in myosin associated with ATP hydrolysis revealed with a fluorescent probe linked directly to the sulfur atom. *J. Biol. Chem.* **268**, 24742-24750
26. Hitatsuka, T. (1992) Movement of Cys697 in myosin ATPase associated with ATP hydrolysis. *J. Biol. Chem.* **267**, 14941-14948
27. Reisler, E. (1982) Sulfhydryl modification and labeling of myosin. *Methods Enzymol.* **85**, 84-93
28. Reisler, E., Burke, M., Himmelfarb, S., and Harrington, W.F. (1974) Spatial proximity of the two essential sulfhydryl groups of myosin. *Biochemistry* **13**, 3837-3840
29. Wells, J.A. and Yount, R.G. (1982) Chemical modification of myosin by active-site trapping of metal-nucleotides with thiol crosslinking reagents. *Methods Enzymol.* **85**, 93-116
30. Cheung, H.C., Gryczynski, I., Malak, H., Wiczk, W., Johnson, M.L., and Lakowicz, J.R. (1991) Conformational flexibility of the Cys697-Cys707 segment of myosin subfragment-1. Distance distributions by frequency-domain fluorometry. *Biophys. Chem.* **40**, 1-17
31. Kubo, S., Tokura, S., and Tonomura, Y (1960) On the active site of myosin A—Adenosine triphosphate. *J. Biol. Chem.* **235**, 2835-2839
32. Miyanishi, T., Inoue, A., and Tonomura, Y. (1979) Differential modification of specific lysine residues in the two kinds of subfragment-1 of myosin with 2,4,6-trinitrobenzenesulfonate. *J. Biochem.* **85**, 747-753
33. Setton, A. and Muhlrad, A. (1988) The effect of pyrophosphate on the reaction of myosin with 2,4,6-trinitrobenzene sulphonate. *J. Muscle Res. Cell Motil.* **9**, 132-146
34. Maruta, S., Henry, G.D., Ohki, T., Kambara, T., Sykes, B.D., and Ikebe, M. (1998) Analysis of stress in the active site of myosin accompanied by conformational changes in transient state intermediate complexes using photoaffinity labeling and ^{19}F-NMR spectroscopy. *Eur. J. Biochem.* **252**, 520-529
35. Park, S., Ajtai, K., and Burghardt, T.P. (1998) Inhibition of myosin ATPase by metal fluoride complexes. *Biochim. Biophys. Acta*, in press
36. Henry, G.D., Maruta, S., Ikebe, M., and Sykes, B.D. (1993) Observation of multiple myosin subfragment 1-ADP-fluoroberyllate complexes by ^{19}F NMR spectroscopy. *Biochemistry* **32**, 10451-10456
37. Maruta, S., Homma, K., and Ohki, T. (1998) Conformational changes at the highly reactive cystein and lysine regions of skeletal muscle myosin induced by formation of transition state analogues. *J. Biochem.* **124**, 578-584
38. Craig, R., Green, L.E., and Eisenberg, E. (1985) Structure of the actin-myosin complex in the presence of ATP. *Proc. Natl. Acad. Sci. USA* **82**, 3247-3251
39. Katayama, E. (1989) The effects of various nucleotides on the structure of actin-attached myosin subfragment-1 studied by quick-freeze deep-etch electron microscopy. *J. Biochem.* **106**, 751-770
40. Tokunaga, M., Sutoh, K., and Wakabayashi, T. (1991) Structure and structural change of the myosin head. *Adv. Biophys.* **27**, 157-167
41. Uyeda, T.Q.P., Abramson, P.D., and Spudich, J.A. (1996) The neck region of the myosin motor domain acts as a lever arm to generate movement. *Proc. Natl. Acad. Sci. USA* **93**, 4459-4464